ORIGINAL ARTICLE

^{18}F-sodium fluoride PET/CT provides prognostic clarity compared to calcium and Framingham risk scoring when addressing whole-heart arterial calcification

Olivia Sorci[1] · Alexandra S. Batzdorf[1] · Michael Mayer[1] · Sylvia Rhodes[1] · Matthew Peng[1] · Amanda R. Jankelovits[1] · Julia N. Hornyak[1] · Oke Gerke[2] · Poul Flemming Høilund-Carlsen[2] · Abass Alavi[1] · Chamith S. Rajapakse[1,3,4] ⬤

Abstract

Aims To investigate the benefit of utilizing ^{18}F-sodium fluoride (NaF) PET/CT over calcium and Framingham scoring for potential preventative coronary artery disease (CAD) intervention.

Methods and results This retrospective study included 136 participants (ages 21–75, BMI 18–43 kg/m^2): 86 healthy controls and 50 patients. CT heart segmentations were superimposed onto PET images and standard uptake values (SUV) were calculated by a semi-auto segmentation method of drawing volumes of interest around the heart. Intergroup comparisons were made matching 37 patient/control pairs based on age, gender, and BMI. ROC curves were generated to determine how well SUV and Framingham methods predicted patient status. Regressions including all 136 participants were performed between SUV, age, and BMI. Patients exhibited higher average SUV (SUV$_{mean}$; $P = 0.006$) and Framingham scores ($P = 0.02$) than controls. However, ROC curves indicated that SUV$_{mean}$ could discriminate patients from controls (AUC = 0.63, $P = 0.049$), but Framingham scores could not (AUC = 0.44, $P = 0.38$). Calcium scores and maximum SUV (SUV$_{max}$) did not differ between patients and controls. SUV$_{mean}$ correlated with age and BMI among females (age, partial $R^2 = 0.16$, $P = 0.001$; BMI, partial $R^2 = 0.12$, $P = 0.004$) and males (age, partial $R^2 = 0.28$, $P < 0.0001$; BMI, partial $R^2 = 0.22$, $P < 0.0001$).

Conclusion Unlike calcium scores, NaF PET/CT-derived values differed between patients and controls. Framingham risk score patterns echoed those of SUV$_{mean}$, but were not sensitive enough to predict patient status. SUV$_{mean}$ values increased with age and BMI. Therefore, incorporation of NaF PET/CT into routine prognostic CAD assessment might prove beneficial for assessing early stage plaque calcification in coronary arteries.

Trial registration ClinicalTrials.gov (NCT01724749).

Keywords Atherosclerosis · Coronary artery disease · PET/CT · 18F-NaF · Calcification

✉ Chamith S. Rajapakse
   chamith@pennmedicine.upenn.edu

Olivia Sorci
osorci@sas.upenn.edu

Alexandra S. Batzdorf
batzdorf@pennmedicine.upenn.edu

Michael Mayer
michael.mayer@pennmedicine.upenn.edu

Sylvia Rhodes
sylvr@sas.upenn.edu

Matthew Peng
mattpeng@sas.upenn.edu

Amanda R. Jankelovits
amjank@nursing.upenn.edu

Julia N. Hornyak
jhornyak@sas.upenn.edu

Oke Gerke
oke.gerke@rsyd.dk

Poul Flemming Høilund-Carlsen
pfhc@rsyd.dk

Abass Alavi
Abass.Alavi@uphs.upenn.edu

Extended author information available on the last page of the article

Background

Coronary artery disease (CAD) is a condition characterized by plaque deposition and luminal obstruction in the arteries of the heart. This can occur in the main coronary arteries: left coronary artery (LCA), right coronary artery (RCA), and left descending artery (LDA), or in the minor coronary arteries known as microcalcifications. The disease affects one-third of women and one-half of men in their lifetimes [1, 2]. An American will have a coronary event approximately every 25 s and one will die of one every minute [2]. Early prognostic assessment of this disease is therefore crucial to achieve adequate care and good quality of life [2–4].

> Current prognostic modalities to assess coronary artery calcification include calcium scoring and Framingham risk scoring. Diagnostic methods include stress echocardiography, coronary CT angiography (CCTA), myocardial perfusion imaging utilizing single-photon emission computed tomography (CT) or ultrasound, and cardiovascular magnetic resonance [5].

There are other ways of assessing CAD, but the methodologies listed above represent the main imaging modalities in current use. In addition, the structural methodology of coronary artery calcium scoring (CAC), along with lifestyle measurements and blood chemistry values, can be the primary factor when measuring risk in asymptomatic patients [6]. A lack of consensus exists when considering the strength of association between CAC scores and adverse coronary events [6, 7]. Some studies suggest CAC scores are appropriate for assessing individuals with intermediate CAD risk but prove less beneficial when addressing those at low risk [6–8]. While CAC has been traditionally quantified using the Agatston scoring method and has prognostic value in large populations, it has several limitations [6].

CAC scoring can be conducted in various ways. Agatston scoring involves using a weighted value assigned to the densest voxel of a given coronary artery. Density is measured in Hounsfield units and an Agatston density score of 1 corresponds with 130–199 HU, 2 with 200–299 HU, 3 with 300–399 HU, and 4 with 400–499 HU or greater [6]. The weighted score is then multiplied with the area (in millimeters) of the calcification. Mass- and volume-based measurements also exist where the actual and mass and volume are measured in the artery being examined [6, 7]. Given the "stepwise" classification of the density Agatston score, this method may not examine subtle changes to coronary artery calcification.

Framingham risk scoring is focused on assessing future coronary events. This method estimates the 10-year CAD risk of an individual on the basis of various criteria including cholesterol, age, gender, and systolic blood pressure [8, 9]. Framingham scoring uses variables known to increase CAD to determine the likelihood of a coronary event, but it does not provide physiological evidence of calcified plaque or predict how quickly CAD will progress.

Calcified plaque therefore presents a great challenge to clinicians and radiologists as numerous methods exist to analyze calcification for prevention and treatment purposes, all with different strengths of association in determining risk for a coronary episode.

The exceedingly small scale of microcalcification lesions occupying arteries makes identification a serious challenge when using customary imaging techniques such as X-ray angiography, CT angiography, and calcium scoring. Using ^{18}F-sodium fluoride (NaF) PET/CT imaging is a promising tool used in conjecture with other techniques; potentially assessing early coronary calcification because it allows for measurement of biologically active plaque in which the quantity of radiotracer absorbed is directly correlated with the amount of calcified plaque existent in the vasculature [9–16].

The purpose of our study was to investigate the usefulness of NaF standard uptake value(SUV), as compared to calcium and Framingham risk scores; two methods heavily validated in the literature as providing a strong predictive value of a coronary event [5–8]. Ideally, NaF will serve as a biomarker of microcalcification in the coronary arteries for [1] identifying patients with persistent chest pain and [2] quantifying age- and BMI-related increases in calcified plaque content.

Materials and methods

Our participants for this retrospective study were taken from the larger prospective Cardiovascular Molecular Calcification Assessed by NaF PET/CT (CAMONA) study conducted by Odense University Hospital (10–12, 17). The CAMONA study was approved by the DanishNational Health Committee on Health Research Ethics, registered at ClinicalTrials.gov (NCT01724749) and conducted in accordance with the Declaration of Helsinki. All participants provided written informed consent.

Participant selection

The CAMONA study recruited participants for a prospective heart study. Of the 139 total participants, 89 were designated as healthy controls and 50 were patients who had been referred for coronary CT angiography on the basis of persistent chest pain. Angina in the patient population was present before CCTA referral, but the duration of chest pain before referral is not known. Three healthy controls did not have necessary PET/CT images on file for our analysis, resulting in 86 control participants. Included in the study were 68 females (ages 21–75, BMI 18–37 kg/m^2) and 68 males (ages 23–75 years, BMI 18–43 kg/m^2).

Inclusion criteria for healthy controls included systolic blood pressure below 160 mm/Hg with diastolic blood pressure below 100 mm/Hg, glycated hemoglobin below 48 mmol/mol, and total serum cholesterol below 6.2 mmol/L. Patient groups were also required to meet this criterion in addition to the angina they experienced upon referral for angiography. Individuals with a history of smoking and diagnosis of type II diabetes were not eligible for inclusion. Previous history of any cardiovascular events (i.e., acute myocardial infarction, transient ischemic attack, and ischemic stroke), cancer, chronic inflammatory disease, or kidney failure was eligible for exclusion. These patients are already at increased cardiovascular risk and are less likely to benefit from vascular calcification imaging with PET. Additionally, only patients with a 10-year risk for fatal cardiovascular disease equal to or above 1%, as estimated by the body mass index (kg/m2)–based Systematic Coronary Risk Evaluation (SCORE) tool, were eligible for inclusion.

All 136 participants were used to examine associative variables (i.e., age, BMI, SUV). Intergroup SUV comparisons—between patients and controls—utilized 37 pairs matched on the basis of age ($\pm$ 6 years), gender, and BMI ($\pm$ 3.2 kg/m^2) to help minimize variables that could potentially influence CAD risk and manifestation. By controlling for these variables, we could directly compare diagnostic methods for detecting plaque deposition in similar cohorts with an already known diagnostic conclusion—whether they qualify as patients or controls.

Unless otherwise specified, data are means $\pm$ SD. Patients did not differ from paired controls in gender, height, weight, dosage, or age

Study design

NaF PET/CT imaging was performed on hybrid PET/CT machines under the same conditions for all individuals (GE Discovery STE, VCT, RX, and 690/710). Images were obtained 90 min after intravenous injection of 2.2 MBq of NaF per kilogram of body weight. CT images (140 kV, 30–110 mA, noise index 25, 0.8 s per rotation, slice thickness 3.75 mm) were attenuation corrected. PET images were corrected for scatter and random coincidence.

Body weight, BMI, height, and age were also determined for all participants. Smoking habits, hypertension treatment, and blood analyses including fasting serum total cholesterol, LDL and HDL cholesterol, serum triglycerides, fasting glucose and glycated hemoglobin (HbA1c), and systolic blood pressure were measured to calculate a Framingham risk score for each participant. Comparison analyses were conducted between patients and controls to determine if these blood chemistry values were significant between groups.

Unless otherwise specified data are means $\pm$ SD. Patients differed from controls in total cholesterol, homocysteine, fasting plasma glucose, HbA1c, and eGFR

Calcium scores were determined by multiplying the area of calcium-containing pixels over 130 HU by weight (milligram) to quantify the amount of calcified plaque. Regions of calcified plaque were identified by two radiologists.

Quantitative imaging analysis

SUV was calculated using the operator-guided computer software PMOD (PMOD

Technologies LLC, Switzerland). CT and PET images for each participant were uploaded onto the software and manipulated to create regions of interest (ROIs) on each CT image slice. This was done by segmenting regions around the heart on each 3.75-mm thick coronal slice, moving anteriorly to posteriorly. These ROIs were then stacked to create 3D volumes of interest (VOIs). The VOIs encompassed only the vascular tissue of the heart—blood and the surrounding thoracic cavity were excluded by setting a threshold with a lower limit of -50 HU (Fig. 1). The VOIs were generated using the CT images for structural clarity, then superimposed on the corresponding PET images. From here, average SUV (SUV_{mean}) and maximum SUV (SUV_{max}) were calculated within each VOI.

In order to control for potential alteration of SUV by circulating blood within the heart chambers, a singular ROI was generated in the superior vena cava (SVC). Anatomically, this ROI was automatically traced with a radius of 3.5 mm near the base of the SVC, where it connects to the right atrium (RA). A radius of 3.5 mm was chosen to avoid capturing any of the venous wall, which could also alter SUV. To control for blood pooling, SVC values were set as controls in R version 3.5.1. statistical software when calculating regression analyses between associating variables.

Statistical analysis

Statistical significance was set at $\alpha = 0.05$. All analyses were performed using R version

(R Foundation for Statistical Computing, Vienna, Austria)

Intergroup analyses Thirty-seven matched patient-control pairs were generated. Patients and healthy controls were matched based on age, gender, and BMI to investigate differences in SUV between individuals with persistent chest pain and their control counterparts. Comparative analyses were run between these 37 matched pairs. Paired *t* tests were conducted to determine differences in SUV, Framingham scores, and calcium scores between patients and healthy controls. For measures with significant differences between paired patients

Fig. 1 Volume of interest (VOI) capturing a representative heart. VOIs were thresholded to exclude voxels under − 50 HU before being superimposed onto corresponding PET images
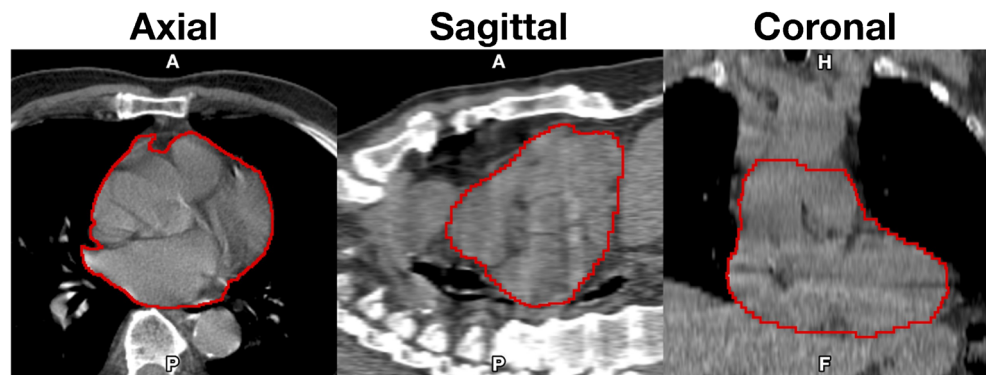
and controls, receiver operator characteristic (ROC) curves were generated to determine how well these measures predict patient status by plotting true positive rate against false positive rate. Areas under theROC curves (AUC) were calculated, then evaluated using one-sample Wilcoxon tests.

Full set analyses Multiple regression analyses were performed to determine the association between age and SUV, controlling for BMI, SVC, and dosage, as well as between BMI and SUV, controlling for age, SVC, and dosage. Measures of both SUV_{mean} and SUV_{max} were utilized. Similarly, regressions were performed using CT-derived values, as quantified using HU. These regressions investigated the association between age and HU, controlling for BMI and radiotracer dosage, as well as between BMI and HU, controlling for age and dosage. Male and female regressions were conducted separately but final regression calculations included all 136 subjects.

Results

Intergroup analyses

Participant characteristics Patients did not differ substantially from paired controls in gender, height, weight, dosage, or age (Table 1).

Comparing patients to controls Despite having similar HU values (0.88 HU lower among patients, CI − 3.05–1.30, P = 0.42), compared to matched controls, patients had higher SUV_{mean} (0.09 g/mL higher among patients, CI 0.03—0.15, P = 0.01), but not SUV_{max} (0.04 g/mL lower among patients, CI − 1.06–0.98, P = 0.94; Fig. 2), which was quite noticeable visually (Fig. 3). Patients also had higher 10-year Framingham Risk Scores (2.45 higher among patients, CI 0.46–4.45, P = 0.02; Fig. 4). However, no differences were detected between patients and healthy controls on any calcium score measure (calcium mass, 58 mg lower among patients; CI − 481.93–365.93, P = 0.75; calcium volume, 65.71 mm lower among patients; CI − 458.34–

326.91, P = 0.70; calcium score, 69 AU lower among patients; CI − 622.25–484.25, P = 0.77; Fig. 5).

Although patients exhibited both higher Framingham scores and higher SUV_{mean} than controls, only SUV_{mean} (AUC = 0.63, u = 501.5, CI − 0.15-− 0.0003, P = 0.049), and notFramingham scores (AUC = 0.44, u = 602, CI − 4.20–1.70, P = 0.38), was able to predict patient status (Fig. 6). The data-driven optimal SUV_{mean} cutoff point was determined to be 0.76 g/mL, such that healthy controls' SUV_{mean} < 0.76 g/mL < patients' SUV_{mean} (Table 2).

Full set analyses

Adjusted values of age, controlling for BMI, SVC, and radiotracer dosage, and adjusted values of BMI, controlling for age, SVC, and radiotracer dosage, were both positively correlated with SUV_{mean} among females (age, partial R^2 = 0.16, P = 0.001; BMI, partial R^2 = 0.12, P = 0.004) and males (age, partial R^2 = 0.28, P < 0.0001; BMI, partial R^2 = 0.22, P < 0.0001), while SUV_{max} only correlated with BMI among males (age, partial R^2 = 0.001, P = 0.84; BMI, partial R^2 = 0.17, P = 0.001) and did not correlate with anything among females (age, partial R^2 = 0.01, P = 0.34; BMI, partial R^2 = 0.02, P = 0.27; Fig. 7). Furthermore, no interaction was found in either SUV model between age and gender (SUV_{mean}, ΔR^2 = 0.08, P = 0.30; SUV_{max}, ΔR^2 = 0.01, P = 0.38) or between BMI and gender (SUV_{mean}, ΔR^2 = 0.07, P = .71; SUV_{max}, ΔR^2 = 0.02, P = 0.15).

Table 1 Comparison of patients and matched controls

Parameter	Patients (n = 37)	Controls (n = 37)	P value
Gender (No.)	Female = 18 Male = 19	Female = 18 Male = 19	
Height (m)	1.72 ± 0.09	1.71 ± 0.09	0.66
Weight (kg)	80.65 ± 16.02	77.49 ± 14.64	0.11
Dose (MBq)	171.19 ± 28.99	168.08 ± 37.56	0.67
Age (years)	54.19 ± 11.15	53.60 ± 9.88	0.20

Fig. 2 **a** Patients had significantly higher SUV_{mean} than did healthy controls, but **b** there was no difference in SUV_{max} between patients and controls. Midline represents mean, box represents SD, and whiskers represent range
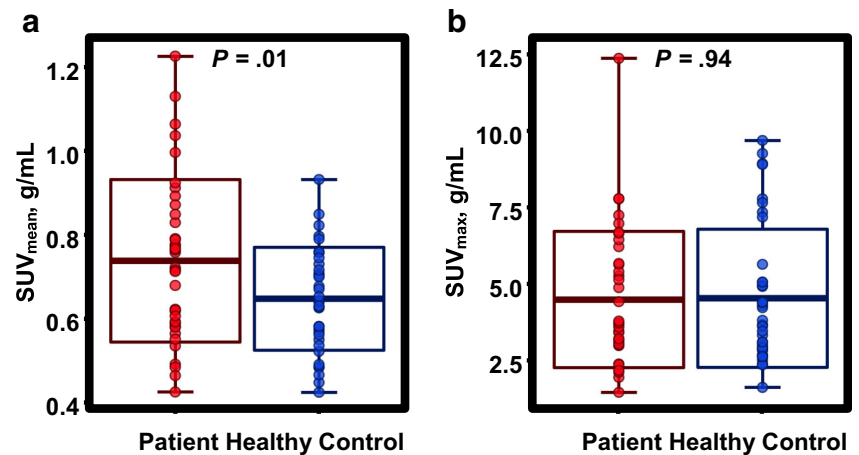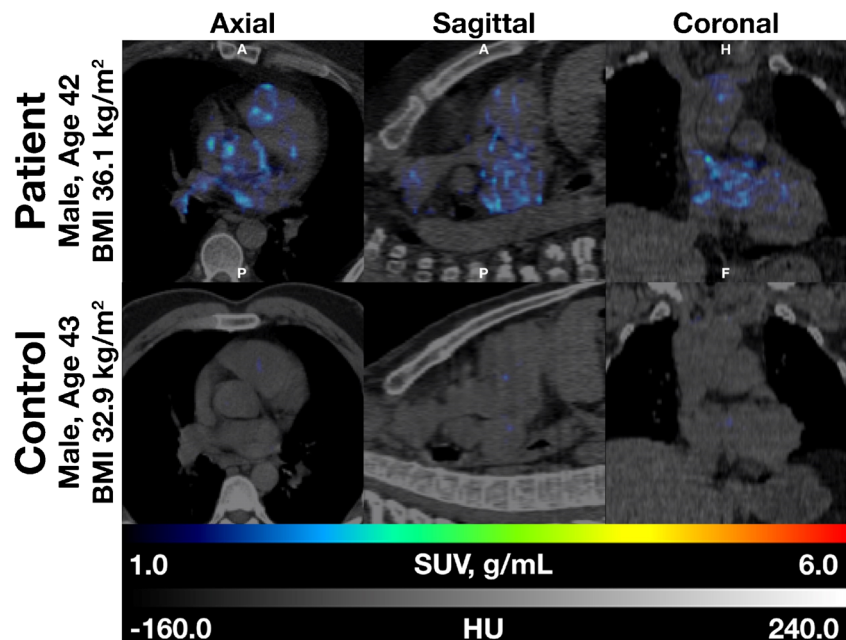
CT-derived HU, however, was not correlated with adjusted values of age among females (partial $R^2 = 0.03$, $P = 0.18$) or males (partial $R^2 = 0.0001$, $P = 0.94$), although adjusted BMI was negatively correlated with HU among females (partial $R^2 = 0.08$, $P = 0.03$) and males (partial $R^2 = 0.24$, $P < 0.0001$). As was the case in the SUV models, there was no interaction between age and gender ($\Delta R^2 = 0.02$, $P = 0.39$) or between BMI and gender ($\Delta R^2 = 0.01$, $P = 0.88$) within the HU models.

Reproducibility

To evaluate the validity of our methodology, 5 researchers conducted segmentation analysis using the methods described above for five study participants. The mean CV and ICC for the inter-operator reproducibility were 1.9% (1.4% to 2.3%) range and 0.997%, respectively.

Discussion

Our study found that SUV_{mean} was positively correlated with both age and BMI, two indicators of coronary artery calcification, among males and females. Compared to matched healthy controls, patients had significantly higher SUV_{mean} and Framingham risk scores. There were no significant differences between matched patients and controls in any calcium scoring method (i.e., mass, volume, Agatston) or in SUV_{max}. The NaF PET/CT SUV_{mean} ROC curve displayed a high degree of accuracy as a predictive method of coronary calcification, while the Framingham risk assessment score did not.

The only pattern detected by SUV_{max} was a significant, positive correlation with BMI among males. This discrepancy between SUV measures is likely because CAD severity is determined more by the overall amount of plaque than by the metabolism of any one particular microcalcification.
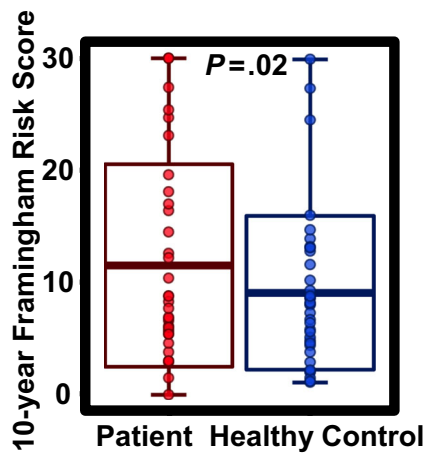
Fig. 3 Fused PET/CT example of (top) a 42-year-old male patient with a BMI of 36.1 kg/m² and (bottom) the corresponding matched control, a 43-year-old male with a BMI of 32.9 kg/m². The patient displays greater radiotracer uptake, indicated by colored pixel intensity

Fig. 4 Patients had significantly higher 10-year Framingham scores than did healthy controls. Midline represents mean, box represents SD, and whiskers represent range

Fig. 6 SUV_{mean}, but not Framingham scores, accurately predicted patient status. SUV_{mean} data-driven optimal cut-off point: 0.76 g/mL. TPR = true positive rate, FPR = false positive rate, FRS = Framingham risk score

Given the popularity of SUV_{max} in NaF PET/CT atherosclerotic plaque detection, the sensitivity of this measure warrants further investigation.

Blood pooling in heart chambers could affect SUV values. Therefore, an ROI of the superior vena cava (SVC) was drawn manually, avoiding the venous wall, to calculate SUV of the blood. Blood SUV can either be included as a variable in
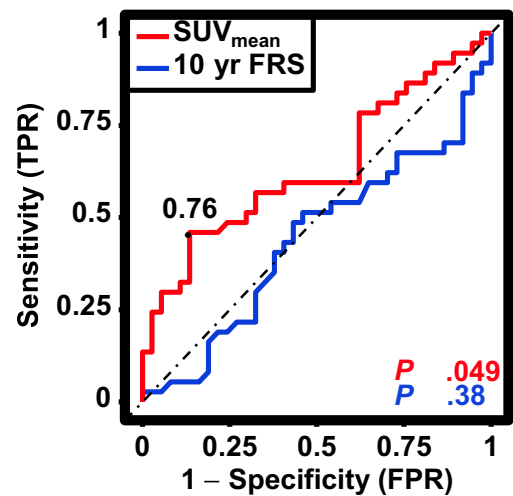
multivariate linear regression or divided by coronary SUV directly to yield a target-to-background ratio (TBR). SVC SUV was utilized as a variable in the multivariate linear regression analyses in this study as it produced stronger correlation with age, BMI, and SUV associations. Further

Fig. 5 Patients and controls had similar **a** calcium masses, **b** calcium volumes, and **c** overall calcium scores. Midline represents mean, box represents SD, and whiskers represent range
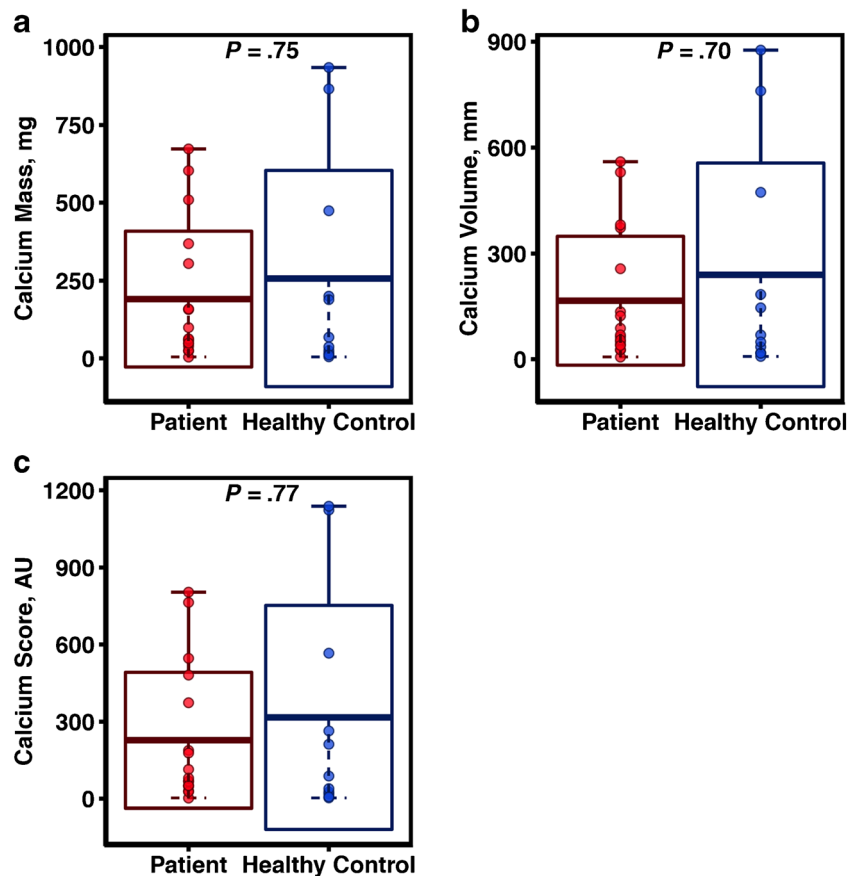
Table 2 Patient and control blood chemistry values

| Average blood chemistry levels	Controls ($n = 86$)	Patients ($n = 51$)	P value
Syst. BP (mmHg)	127.8 ± 17.04	131.1 ± 17.04	0.28
Diast. BP (mmHg)	76.7 ± 10.37	79.2 ± 7.79	0.10
Pulse (beats/min.)	64.6 ± 12.63	64.7 ± 12.30	0.98
Total cholesterol (mmol/L)	4.9 ± 0.86	5.3 ± 0.96	0.01*
LDL cholesterol (mmol/L)	3.1 ± 0.79	3.4 ± 0.88	0.06
HDL cholesterol (mmol/L)	1.4 ± 0.45	1.4 ± 0.43	0.99
Triglycerides (mmol/L)	1.05 ± 0.65	1.2 ± 0.72	0.21
Homocysteine (umol/L)	8.8 ± 2.2	10.5 ± 3.99	0.01*
Fasting plasma glucose (mmol/L)	5.5 ± 0.50	5.9 ± 0.87	0.01*
HbA1c (mmol/mol)	33.9 ± 4.10	37.4 ± 4.98	< 0.0001*
CRP (mg/L)	2.2 ± 2.98	2.6 ± 3.48	0.45
Fibrinogen (umol/L)	10.8 ± 10.7	10.2 ± 2.15	0.64
White blood cell count (cells/L)	6.0 ± 1.80	6.4 ± 2.10	0.26
Creatinine (umol/L)	79.1 ± 13.12	82.8 ± 20.72	0.27
eGFR (mL/min/1.73 m2)	82.9 ± 13.10	75.8 ± 14.94	0.0069*

consideration of how blood circulation influences uptake values would likely result in a more accurate measure of SUV in anatomical vasculature.

Despite the use of prognostic modalities which serves as preventative assessments of coronary calcification and risk of coronary events, there are still 1.5 million acute myocardial infarctions in the USA every year. Calcium scoring, along with X-ray and CT angiography, is the method most commonly utilized by clinicians in acute/emergency settings to assess coronary artery plaque manifestation [5, 18]. Often, calcification assessments occur after patients exhibit severe symptoms, such as chest pain, and are being assessed for revascularization [18]. However, coronary artery plaque and subsequent coronary artery disease (CAD) is often asymptomatic for years and requires a method to analyze small changes in plaque manifestation. Calcium scoring has been validated in some studies as sufficient for determining risk in asymptomatic patients [6, 7, 18–22], yet limitations still exist. Agatston scoring is not conducive to radiation dose reduction which reconstructs images to reduce noise with changing voltage (kVp) and current measurements (mA). This reconstruction will alter pixel dimensions and can cause Agatston miscalculations of 3 to 31% [18]. Functional imaging such as SPECT and MR perfusion tests are beneficial for patients that require prolonged diagnostic intervention and monitoring, but the addition of NaF PET/CT as a methodology for monitoring coronary calcification over an extended period of time could prove beneficial. This is because, unlike functional imaging, which examines hemodynamic changes in response to stress, NaF measures subtle changes in the amount of calcium in the arteries [20–25].

Many of the procedures that diagnose and monitor coronary plaque deposition are invasive and are often limited to

acute coronary events [1, 18, 20]. Coronary computed tomography angiography (CCTA), X-ray angiography, and intravascular ultrasound monitor the amount of calcification in the vessels, and are therefore often a better assessment of disease burden than of near coronary event risk [18]. Arterial stenosis does not correlate with risk of an event. Single-photon emission computed tomography (SPECT) is a functional assessment to determine how the heart responds with added stressors, often exercise or an adenosine injection to mimic exercise's effects. No quantification of plaque in the arteries results from this method. The benefits of ^{18}F-NaF PET/CT imaging in the context of current available imaging modalities is that it provides a way for clinicians to quantify subtle changes in plaque deposition that are not visible to the human eye (picomolar tissue concentrations). Early vascular calcification (microcalcification) in response to inflammation can be detected by NaF below CT resolution [26–31]. It is a method that is less invasive than angiography. NaF PET/CT imaging utilizes a biochemical method and offers quantitative measurement of calcified plaque in the coronary arteries [10–12, 17, 32–34]. This method bypasses the need for subjective recognition with the naked eye by a radiologist, which may explain why calcium scores did not differ between patients and controls [12, 17]. Our methodology for calculating SUV only relied on the eyes of the technician for gross anatomic identification. A preliminary circle was drawn around the heart with the only requirement being that no outside bone or soft tissue be present in the VOI. Then, the VOI was automatically segmented using PMOD software to include HU values that were above a specific threshold of − 50 HU. Even computer-derived CT values obtained from this segmentation did not differ between patients and controls or correlate with age or BMI. This suggests that NaF's utilization of a

Fig. 7 Among females and males, both **a** age, adjusted for BMI and dosage, and **c** BMI, adjusted for age and dosage, were positively correlated with SUV$_{mean}$. **b** Adjusted age was not correlated with SUV$_{max}$ among females or males, while **d** adjusted BMI was positively correlated with SUV$_{max}$ among males, but not females
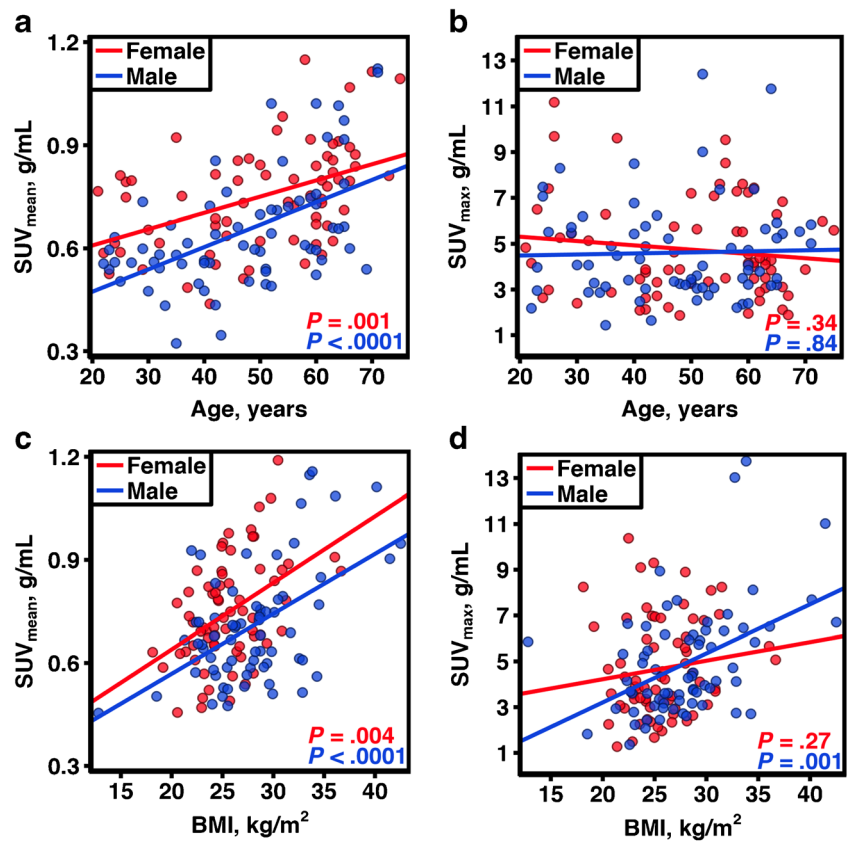
functional pathway renders it sensitive to the formation of microcalcification long before it becomes detectable calcification.

NaF allows for early detection of atherosclerotic plaque because it exchanges a fluoride ion with a hydroxyl group of the accumulated hydroxyapatite in the coronary arteries [35, 19]. SUV$_{mean}$ is effective regardless of whether the plaque is visible to the human eye, or even to computer software, which makes it a promising tool since coronary plaque can be clinically asymptomaticfor years [35].

NaF elucidates functional pathways and is highly sensitive to small changes in plaque accumulation over short periods of time, which makes it ideal for monitoring medication response. However, it has low spatial resolution [35], so it can be difficult to diagnose the loci of plaque deposition accurately in the small coronary arteries. Additionally, NaF is a radiotracer that is best absorbed by bone or "bone-like" material, so atherosclerosis due to an inflammatory response consisting of macrophage infiltration and thrombus generation would not be detected until the plaque becomes calcified [2, 34]. In the future, pairing NaF with FDG, a radiotracer that metabolically interacts with inflammation, could therefore prove beneficial to measure various types of plaque in the arteries so as to obtain a more holistic image of a patient's health.

The limitations of our study include usage of fused PET/CT images previously provided by the scanner without

additional registration to account for fusion error. This could potentiate miscalculations in SUV if CT and PET images do not line up exactly. However, our methodology allows for such a large VOI calculation of the entire heart, in comparison to segmenting individual arteries, potential shifts in fused images would not result in great SUV delineation. In addition, our methodology utilizes a semi-automated method and still relies partially on an operator that draws an initial VOI around the heart. Despite this, our method has a high inter-operatory reproducibility value with minimal deviation in SUV calculations between operators. This study utilizes the CAMONA cohort where neither patients nor healthy controls had any prior history of heart disease, with patients initially being referred for angiography based on chest pain. It is likely that the cohort does not represent the range of SUV present in individuals with severe/long-term heart disease. This fact does not change the fact the NaF PET/CT SUV was still able to detect subtle changes in microcalcifications in the coronary arteries. The duration of the angina of the individuals in the patient cohort before recruitment to the CAMONA study is not known. Therefore, varying levels of plaque accumulation and risk of cardiac events between individuals is likely.

CAD is the leading cause of death worldwide, contributing to a third of all deaths among individuals over the age of 35 [36]. The disease itself is multifaceted in that it has both lifestyle and genetic causes, and it tends to be accompanied by

various comorbidities that could enhance its progression [35–38]. NaF PET/CT imaging offers additional insight of the progression of coronary plaque and subsequent disease. Incorporating this function-based prognostic imaging modality into a clinical setting could expand awareness of patient health and pave the way for advances in care.

Availability of data and material The datasets used and analyzed in the current study are from the CAMONA cohort and are available from the corresponding author on reasonable request.

Compliance with ethical standards

Conflict of interest The authors declare that they have no conflict of interest.

Ethical approval Not applicable.

Consent for publication The CAMONA study was approved by the Danish National Health Committee on Health Research Ethics, registered at ClinicalTrials.gov (NCT01724749) and conducted in accordance with the Declaration of Helsinki. All participants provided written informed consent.

References

1. Irkle A, Vesey AT, Lewis DY, Skepper JN, JLE B, Dweck MR, et al. Identifying active vascular microcalcification by 18F-sodium fluoride positron emission tomography. Nature Communications. 2015;6(1).
2. Fleg JL, Stone GW, Fayad ZA, Hatsukami GJF, TS KF, Ohayon J, et al. Detection of high-risk atherosclerotic plaque: report of the NHLBI Working Group on current status and future directions. JACC Cardiovasc Imaging. 2012;5(9):941–55.
3. Roger VL, Go AS, Lloyd-Jones DM, Adams RJ, Berry JD, Brown TM, et al. Heart disease and stroke statistics–2011 update: a report from the American Heart Association. Circulation. 2011;123(4):18–209.
4. Lloyd-Jones D, Adams RJ, Brown TM, Carnethon M, Dai S, De Simone G, et al. Executive summary: heart disease and stroke statistics—2010 update: a report from the American Heart Association. Circulation. 2010;121(7):948–54.
5. Siontis GC, Mavridis D, Greenwood JP, Coles B, Nikolakopoulou A, Jüni P, et al. Outcomes of non-invasive diagnostic modalities for the detection of coronary artery disease: network meta-analysis of diagnostic randomised controlled trials. BMJ. 2018.
6. Malguria N, Zimmerman S, Fishman EK. Coronary artery calcium scoring. Journal of Computer Assisted Tomography. 2018;42(6):887–97.
7. Willemink MJ, Werf NRVD, Nieman K, Greuter MJ, Koweek LM, Fleischmann D. Coronary artery calcium: a technical argument for a new scoring method. Journal of Cardiovascular Computed Tomography. 2018.
8. Rumberger JA, Kaufman L. A rosetta stone for coronary calcium risk stratification: Agatston, volume, and mass scores in 11,490 individuals. AJR Am J Roentgenol. 2003;181(3):743–8.
9. Ulzheimer S, Kalender WA. Assessment of calcium scoring performance in cardiac computed tomography. Eur Radiol. 2003;13(3):484–97.
10. Blomberg BA, Thomassen A, Takx RAP, Vilstrup MH, Hess S, Nielsen AL, et al. Delayed sodium 18F-fluoride PET/CT imaging does not improve quantification of vascular calcification metabolism: Results from the CAMONA study. Journal of Nuclear Cardiology. 2013;21(2):293–304.
11. Blomberg BA, Thomassen A, Jong PAD, Lam MG, Diederichsen AC, Olsen MH, et al. Coronary fluorine-18-sodium fluoride uptake is increased in healthy adults with an unfavorable cardiovascular risk profile. Nuclear Medicine Communications. 2017;38(11):1007–14.
12. Blomberg BA, Jong PAD, Thomassen A, Lam MGE, Vach W, Olsen MH, et al. Thoracic aorta calcification but not inflammation is associated with increased cardiovascular disease risk: results of the CAMONA study. European Journal of Nuclear Medicine and Molecular Imaging. 2016;44(2):249–58.
13. Dweck MR, Chow MW, Joshi NV, Williams MC, Jones C, Fletcher AM, et al. Coronary arterial 18F-sodium fluoride uptake: a novel marker of plaque biology. J Am Coll Cardiol. 2012;59(17):1539–48.
14. Joshi NV, Vesey AT, Williams MC, Shah AS, Calvert PA, Craighead FH, et al. 18F-fluoride positron emission tomography for identification of ruptured and high-risk coronary atherosclerotic plaques: a prospective clinical trial. Lancet. 2014;383(9918):705–13.
15. Moss AJ, Doris MK, Andrews JPM, Bing R, Daghem M, van Beek EJR, et al. Molecular coronary plaque imaging using (18)F-fluoride. Circ Cardiovasc Imaging. 2019;12(8):e008574.
16. Li L, Li X, Jia Y, Fan J, Wang H, Fan C, et al. Sodium-fluoride PET-CT for the non-invasive evaluation of coronary plaques in symptomatic patients with coronary artery disease: a cross-correlation study with intravascular ultrasound. Eur J Nucl Med Mol Imaging. 2018;45(12):2181–9.
17. Blomberg BA, Thomassen A, Jong PAD, Simonsen JA, Lam MGEH, Nielsen AL, et al. Impact of personal characteristics and technical factors on quantification of sodium 18F-fluoride uptake in human arteries: prospective evaluation of healthy subjects. Journal of Nuclear Medicine. 2015;56(10):1534–40.
18. Tarkin JM, Dweck MR, Evans NR, Takx RAP, Brown AJ, Tawakol A, et al. Imaging atherosclerosis. Circulation Research. 2016;118:750–69.
19. Mortality GBD. Causes of Death C. Global, regional, and national age-sex specific all cause and cause-specific mortality for 240 causes of death, 1990-2013: a systematic analysis for the Global Burden of Disease Study 2013. Lancet. 2015;385(9963):117–71.
20. Tarkin JM, Dweck MR, Evans NR, Takx RAP, Brown AJ, Tawakol A, et al. Imaging atherosclerosis. Circulation Research. 2016;118:750–69.
21. Beheshti M, Saboury B, Mehta NN, Torigian DA, Werner T, Mohler E, et al. Detection and global quantification of cardiovascular molecular calcification by fluoro18-fluoride positron emission tomography/computed tomography–a novel concept. Hell J Nucl Med. 2011;14:114–21.20.
22. Yoon W, Crisostomo P, Halandras P, Bechara C, Aulivola B. The utility of the Agatston calcium score in predicting carotid plaque vulnerability. Annals of Vascular Surgery. 2018;48:6–7.
23. Al-Mallah MH. Coronary artery calcium scoring: do we need more prognostic data prior to adoption in clinical practice. JACC: Cardiovascular Imaging. 2018;11(12):1807–9.
24. Allam AHA, Thompson RC, Eskander MA, Ali MAM, Sadek A, Rowan CJ, et al. Is coronary calcium scoring too late? Total body arterial calcium burden in patients without known CAD and normal MPI. Journal of Nuclear Cardiology. 2017;25(6):1990–8.
25. Derlin T, Wisotzki C, Richter U, Apostolova I, Bannas P, Weber C, et al. In vivo imaging of mineral deposition in carotid plaque using 18F-sodium fluoride PET/CT: correlation with atherogenic risk factors. Journal of Nuclear Medicine. 2011;52(3):362–8.

26. Morbelli S, Fiz F, Piccardo A, Picori L, Massollo M, Pestarino E, et al. Divergent determinants of 18F–NaF uptake and visible calcium deposition in large arteries: relationship with Framingham risk score. The International Journal of Cardiovascular Imaging. 2013;30(2):439–47.

27. Raynor W, Houshmand S, Gholami S, Emamzadehfard S, Rajapakse CS, Blomberg AB, et al. Evolving role of molecular imaging with 18F-sodium fluoride PET/CT as a biomarker for calcium metabolism. Osteoporosis Reports. 2016;4:115–25.

28. Czernin J, Satyamurthy N, Schiepers C. Molecular mechanisms of bone 18F-NaF deposition. Journal of Nuclear Medicine. 2010;51: 1826–9.

29. McKenney-Drake ML, Territo PR, Salavati A, Houshmand S, Persohn S, Liang Y, et al. (18) F-NaF PET imaging of early coronary artery calcification. JACC Cardiovasc Imaging. . https://doi.org/10.1016/j.jcmg.2015.02.026.

30. Marsch E, Sluimer JC, Daemen MJ. Hypoxia in atherosclerosis and inflammation. Curr Opin Lipidol. 2013;24:393–400. https://doi.org/10.1097/MOL.0b013e32836484a4.

31. van der Valk FM, Kroon J, Potters WV, Thurlings RM, Bennink RJ, Verberne HJ, Nederveen AJ, Nieuwdorp M, Mulder WJ, Fayad ZA, van Buul JD, Stroes ES. In vivo imaging of enhanced leukocyte accumulation in atherosclerotic lesions in humans. J Am Coll Cardiol. 2014;64:1019– 1029. https://doi.org/10.1016/j.jacc.2014.06.11.

32. Derlin T, Richter U, Bannas P, Begemann P, Buchert R, Mester J, et al. Feasibility of 18F-sodium fluoride PET/CT for imaging of atherosclerotic plaque. Journal of Nuclear Medicine. 2010;51(6): 862–5.

33. Libby P, Theroux P. Pathophysiology of coronary artery disease. Circulation. 2005;111(25):3481–8.

34. Tiong AY, Brieger D. Inflammation and coronary artery disease. Am Heart J. 2005;150(1):11–8.

35. Hanson MA, Fareed MT, Argenio SL, Agunwamba AO, Hanson TR. Coronary artery disease. Prim Care. 2013;40(1):1–16.

36. Janssen T, Bannas P, Herrmann J, Veldhoen S, Busch JD, Treszl A, et al. Association of linear 18F-sodium fluoride accumulation in femoral arteries as a measure of diffuse calcification with cardiovascular risk factors: a PET/CT study. Journal of Nuclear Cardiology. 2013;20(4):569–77.

37. Barquera S, Pedroza-Tobías A, Medina C, Hernández-Barrera L, Bibbins-Domingo K, Lozano R, et al. Global overview of the epidemiology of atherosclerotic cardiovascular disease. Archives of Medical Research. 2015;46(5):328–38.

38. Wilson P. Established risk factor and coronary artery disease: The Framingham Study. American Journal of Hypertension. 1997;7(7): 7–12.

Affiliations

Olivia Sorci[1] · Alexandra S. Batzdorf[1] · Michael Mayer[1] · Sylvia Rhodes[1] · Matthew Peng[1] · Amanda R. Jankelovits[1] · Julia N. Hornyak[1] · Oke Gerke[2] · Poul Flemming Høilund-Carlsen[2] · Abass Alavi[1] · Chamith S. Rajapakse[1,3,4]

1 Department of Radiology, University of Pennsylvania, Philadelphia, PA, USA

2 Department of Nuclear Medicine, Odense University Hospital, Odense, Denmark

3 Department of Orthopaedic Surgery, University of Pennsylvania, Philadelphia, PA, USA

4 MRI Education Center, 1 Founders Building, 3400 Spruce St., Philadelphia, PA 19104, USA